NeuroImage 256 (2022) 119253

Contents lists available at ScienceDirect

NeuroImage

journal homepage: www.elsevier.com/locate/neuroimage

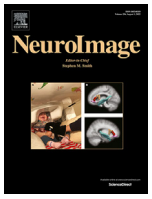

Resting-state functional connectivity of social brain regions predicts motivated dishonesty

Luoyao Pang [a,b,c], Huidi Li [d], Quanying Liu [e], Yue-Jia Luo [b,f,g,**], Dean Mobbs [h], Haiyan Wu [a,*]

[a] Centre for Cognitive and Brain Sciences and Department of Psychology, University of Macau, Taipa, Macao
[b] Center for Brain Disorders and Cognitive Sciences, Shenzhen University, China
[c] College of Psychology and Sociology, Shenzhen University, China
[d] Department of psychology, McGill University, Canada
[e] Shenzhen Key Laboratory of Smart Healthcare Engineering, Southern University of Science and Technology, China
[f] The Research Center of Brain Science and Visual Cognition, Kunming University of Science and Technology, China
[g] College of Teacher Education, Qilu Normal University, China
[h] Division of the Humanities and Social Sciences, California Institute of Technology, USA

ARTICLE INFO

Keywords:
Functional connectivity
Resting-state fMRI
Dishonesty
Machine learning
Predictive modeling
reproducibility

ABSTRACT

Motivated dishonesty is a typical social behavior varying from person to person. Resting-state fMRI (rsfMRI) is capable of identifying unique patterns from functional connectivity (FC) between brain regions. Recent work has built a link between brain networks in resting state to dishonesty in Western participants. To determine and reproduce the relevant neural patterns and build an interpretable model to predict dishonesty, we analyzed two conceptually similar datasets containing rsfMRI data with different dishonesty tasks. Both tasks implemented the information-passing paradigm, in which monetary rewards were employed to induce dishonesty. We applied connectome-based predictive modeling (CPM) to build a model among FC within and between four social brain networks (reward, self-referential, moral, and cognitive control). The CPM analysis indicated that FCs of social brain networks are predictive of dishonesty rate, especially FCs within reward network, and between self-referential and cognitive control networks. Our study offers an conceptual replication with integrated model to predict dishonesty with rsfMRI, and the results suggest that frequent motivated dishonest decisions may require the higher engagement of social brain regions.

1. Introduction

Dishonesty is defined as the act of deliberately concealing the truth or conveying false information, with the purpose of gaining benefits or avoiding loss (Abe, 2011; DePaulo et al., 2003). Although dishonesty is regarded as a violation of the moral code, it is essential for survival and adaptation (Buss, 2019). In the in-lab experiments, according to the experimental manipulation, dishonesty can be divided into two types, instructed dishonesty and motivated (or spontaneous) dishonesty (Wu et al., 2009; Sai et al., 2018). For the former, participants make honest or dishonest responses according to the given instructions (Wu et al., 2009); for the latter, participants usually lie spontaneously under material or monetary incentives (Sai et al., 2018). In developmental psychology, motivated lies have appeared in early childhood (Fu and Lee, 2007). Various motivations drive this kind of dishonesty. For example, people may commit self-serving dishonesty for their own benefit or prosocial dishonesty for the benefit of others. In this study, we focus on motivated dishonesty driven by self-interest to investigate the individual differences and the neural associations underlying it.

Existing task-based fMRI studies have been investigating the neural mechanisms of dishonest behavior (either the instructed dishonesty or the motivated dishonesty) and found that dishonesty is associated with many brain areas, including motivation system, cognitive control system, reward system, moral system and so on. For example, dishonesty with selfish motivations leads to increased striatum activity and stronger FC between valuation and cognitive control networks (Cui et al., 2018; Pornpattananangkul et al., 2018). In contrast, altruistic dishonesty is considered more acceptable and results in decreased anterior insula (AI) activity (Lewis et al., 2012; Yin et al., 2017). Since being dishonest has to inhibit automatic honest responses or resist reward temptation, cognitive control is involved in dishonesty (Bargh and Chartrand, 1999; Greene and Paxton, 2009; Haidt, 2001). Evidence from fMRI studies consistently shows that dishonest responses activate brain regions related to cognitive control, such as the dorsolateral prefrontal cortex (DLPFC),

* Corresponding author at: Center for Brain Disorders and Cognitive Sciences, Shenzhen University, China.
** Co-corresponding author.
E-mail addresses: luoyj@szu.edu.cn (Y.-J. Luo), haiyanwu@um.edu.mo (H. Wu).

https://doi.org/10.1016/j.neuroimage.2022.119253.
Received 7 September 2021; Received in revised form 11 April 2022; Accepted 16 April 2022
Available online 28 April 2022.

the ventrolateral prefrontal cortex (VLPFC), the medial frontal cortex (MFC), and the anterior cingulate cortex (ACC) (Christ et al., 2009; Farah et al., 2014). Moreover, as the reward is usually employed to motivate individuals to lie, outcomes of successful dishonest choices elicit stronger activation in the reward system, such as the ventral striatum and posterior cingulate cortex (PCC) (Sun et al., 2015). Interestingly, the neural response to anticipated reward in the nucleus accumbens (NAcc) can significantly predict dishonest behavior in an incentivized prediction task (Abe and Greene, 2014), indicating that the expectation of reward is critical in motivated dishonesty. In addition to the above processes, morality and self-reference may act as modulators in the middle. For example, participants who paid lower costs for harming others have stronger dorsal striatal responses to the profits gained from doing so (Crockett et al., 2017). Compared with the undetected dishonesty paradigm, the sender-receiver paradigm can arouse stronger self-reference due to the presence of the recipient, leading to increased self-evaluation and neural responses in the orbitofrontal cortex (OFC) and prefrontal cortex (PFC) (Cui et al., 2018; Hughes and Beer, 2013; Yin et al., 2017).

Although task-based fMRI can directly locate the brain regions under a specific task, rsfMRI embodies spontaneous neural activity, and the resting-state brain networks obtained by rsfMRI can predict individual differences (Biswal et al., 1995; Raichle, 2011). It has been demonstrated that there is a sizable overlap between one's rsfMRI and task-fMRI(i.e., 80%, see (Biswal et al., 1995)). A recent theory proposed that spontaneous fluctuations of correlated activity within and across brain regions at rest may reflect the most common perceptual, motor, cognitive, and interoceptive states, which are proactive and predictive (Pezzulo et al., 2021). Apart from fundamental cognitive functions (e.g., perception and attention), rsfMRI can also be used to predict complicated social behaviors (Bellucci et al., 2019; Christov-Moore et al., 2020; Li et al., 2013; Shi et al., 2018; Tian et al., 2017). One hot topic is whether the pre-task rsfMRI can be used to predict individual dishonesty. Compared with the task-fMRI, rsfMRI is more convenient in data collection, and the protocol is easier if we are interested in predicting lies in daily life (Bettus et al., 2010; Lin et al., 2018). To this end, we will explore whether brain activity during rsfMRI can predict incentive dishonesty.

The functional connectivity analysis using rsfMRI has been applied to explore individual differences in dishonesty, providing neural insights into the cognitive framework. The cognitive processes (including reward valuation, self-reference, moral regulation, and cognitive control) and their interactions are proved to be the main predictors of the frequency of someone's dishonest behavior (Speer et al., 2020, 2022; Yin et al., 2021). Specifically, for brain regions involved in reward processing such as caudate and NAcc, it has been found that their FC with medial PFC (a key region in self-referential processing) is positively correlated with honesty, which suggests the potential of promoting honesty by incorporating internal value into reward evaluation (Yin et al., 2021). This is consistent with the evidence from another taskbased fMRI study, which suggests that the self-processing network, mainly consisting of mPFC, PCC, and temporoparietal junction (TPJ), may maintain a positive self-image and thereby increase honesty (Speer et al., 2020). Moreover, strengthened FC between self-referential network and cognitive control network may prompt honesty (Speer et al., 2020). In addition, stronger FC between cognitive control network and reward network may be associated with a higher tendency to be dishonest, no direct evidence from rsfMRI studies though (Pornpattananangkul et al., 2018). Although studies have confirmed the contribution of social brain networks (reward, self-referential, moral, and cognitive control) in predicting dishonesty, it is still unclear whether the results could be generalized to different paradigms and different cultures.

One rsfMRI-based approach commonly used for predicting dishonesty is the connectome-based prediction modeling (CPM) (Ren et al., 2021; Shen et al., 2017), which aims to build a brain-behavior relationship through the cross-validated predictive model. To ensure the generalization of the model, two or more independent datasets are usually employed. In this study, we used two datasets with conceptually similar paradigms, one for internal validation, the other for external validation. Recently, a big concern of brain-behavior association is the reproducibility and replicability of these studies (Marek et al., 2022; Klapwijk et al., 2021; Valk et al., 2020). Researchers call for a rather big sample or more replication studies to reveal similar correlations between brain connectivity and human behavior. For example, Marek et al. (2022) argue that reproducible brain-wide association studies require thousands of samples. Therefore, we are also interested in the reproducibility of the link between dishonesty and the related networks proved in Speer et al. (2022). To test our hypothesis with replicable predictive effect on social brain regions, we further explore whether such predictive effect of resting-state FC (rsFC) features in dishonesty prediction would be replicated in two samples in eastern culture, with small sample size and different tasks.

In this study, we used the incentive dishonesty paradigm (information-passing task) and performed comprehensive rsfMRI analyses to explore the relationship between individual variations in dishonest behavior and its neural patterns, especially FCs between social brain regions and networks. In the dishonesty task, we asked participants to send information (food preference or answer of a trivia question) to another player with an assigned reward to motivate participants to pass the true information (honest condition) or to pass the wrong information (dishonest condition). Eight-minute rsfMRI was scanned just before the task. This study mainly focused on: (i) bridging FCs within and between social brain networks (reward, self-referential, moral, and cognitive control) with dishonesty through the CPM analysis (**Section 2.4**); (ii) forming an integrative view of the rsfMRI predictive model for dishonesty based on the findings (See Fig. S1 for the pipeline of the study); (iii) replicating the recent work (Speer et al., 2022) on FCs of networks predicting dishonesty.

2. Methods

2.1. Internal validation dataset

2.1.1. Participants

Thirty-one participants (16 females) participated in the fMRI experiment (age: mean ± *SD* = 23.74 ± 4.08). Two participants were excluded due to excessive head movements (> 2 mm or > 2°). The remaining 29 participants (15 females) ranged from 18 to 39 years old (mean ± *SD* = 23.86 ± 4.16). We recruited participants from the student community at the university. All participants were right-handed and had no history of neurological or psychiatric disorders. Participants gave written informed consent after being provided with a complete description of the study. Participants received full debriefing after the completion of the experiment. All procedures involved were in accordance with the Declaration of Helsinki and were approved by the Institutional Review Board (IRB) of the Institute of Psychology, Chinese Academy of Sciences.

2.1.2. The procedure of the task

The task used in the current dataset was taken from a series of experiments which include seven sessions (see supplementary materials for description of the whole experiment). From the participants' perspective, the whole experiment was about information receiving and passing. For this study, we only focused on session 3 of the experiments (an information-passing task). In this task, the participants played the role of information sender, passing the food preference information to another player (receiver) with consideration of the amount of reward. Although we told participants that the receiver might get more reward units if he or she chooses more correct answers based on the received information, there was no real "receiver" to receive the information, and there was no further interaction between participants and the receiver. In total, we selected 24 pairs of food and randomly chose the

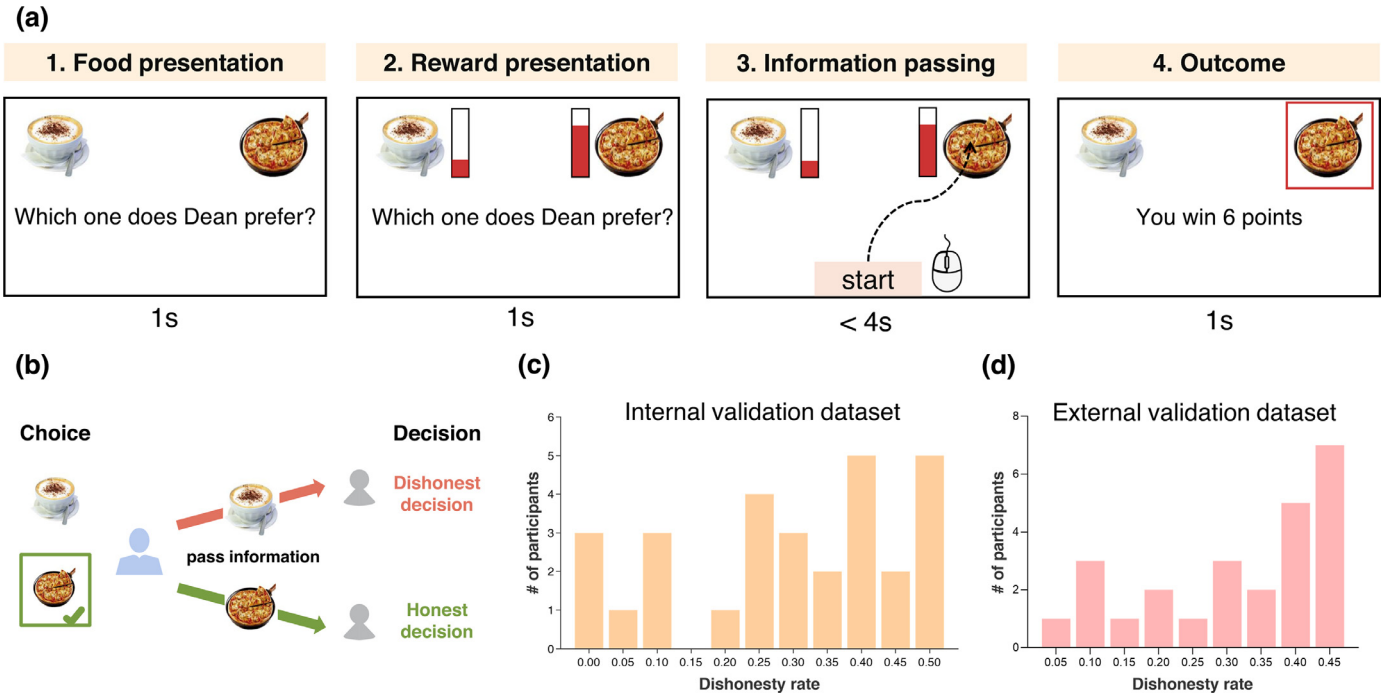

Fig. 1. The information-passing task. (a) A single trial example of the task used in the internal validation dataset. The participant played as an information sender to pass food preference information to another player with consideration of reward units. (b) Possible responses of participants. Honest decision refers to participants passing the true information based on their memory; Dishonest decision refers to participants passing the false information for more rewards. (c) The histogram of dishonesty rate across participants for the internal validation dataset (N = 29). (d) The histogram of dishonesty rate across participants for the external validation dataset (N = 25).

preferred food in each pair. The food images were selected from Food-Pics Extended (http://food-pics.sbg.ac.at). Each participant had a learning session to memorize the list of the preferred food. The dishonesty task would not start unless the accuracy of all 24 pairs of food reached above 90%. Thus participants knew the correct answer for all questions. In each trial (Fig. 1a), the question and two answers were presented for 1 s, and then the reward corresponding to each food was presented on the left and right sides. Participants had to choose an answer within 4 s. The chosen answer and the resulting reward would be highlighted for 1 s. The jitters between trials were 2–8 s (mean = 4 s).

Trials with a higher reward for the true answer were defined as the **honest condition**. In contrast, trials with a higher reward for the wrong answer to motivate dishonesty were defined as the **dishonest condition**. The reward units were drawn from a uniform distribution [2,4,6,8], using pseudo-random sampling with replacement. Both the honest and dishonest conditions consisted of 96 trials separated into four runs. Each pair of food items were repeated eight times, with two times in each run. Possible responses of participants were shown in Fig. 1b. The dishonesty rate was defined as the proportion of false information delivered in the dishonest condition, calculated to measure self-serving lying behavior.

2.1.3. MRI acquisition

MRI data was collected with a General Electric 3T scanner (GE Discovery MR750). The rsfMRI data was collected by an echo-planar imaging (EPI) sequence utilizing gradient echo. Slices were acquired in interleaved order and the data consisted of 200 whole-brain volumes (repetition time (TR) = 2000 ms, echo time (TE) = 21 ms, flip angle = 90°, slice number = 42, slice thickness = 3.5 mm, matrix size = 64 × 64, field of view (FOV) = 200 mm, and voxel size = 3.1 × 3.1 × 3.5 mm^3). T1-weighted structural image data was collected for anatomical reference using a 3D magnetization-prepared rapid gradient-echo (MPRAGE) sequence (TR = 2530 ms, TE = 2.34 ms, flip angle = 7°, FOV = 256 mm, slice number = 176, slice thickness = 1 mm, in-plane matrix resolution = 256 × 256, FOV = 256 mm, and voxel size = 1 × 1 × 1 mm^3).

2.2. External validation dataset

2.2.1. Participants

Twenty-nine healthy participants (14 female; age: mean ± SD = 19.86 ± 3.69) from the University of Macau were recruited by online advertisement. One participant was excluded due to excessive head movements (> 2 mm or > 2°). Three participants were excluded because they remained honest throughout the whole experiment. All participants were right-handed with normal or corrected-to-normal vision and had not participated in any similar studies. All participants signed the informed consent before the formal experiment, and the experimental protocol was approved by the Institutional Review Board of the University of Macau (BSERE21-APP005-ICI). At the end of the study, participants were paid with a 130 - 150 mop supermarket coupon.

2.2.2. The procedure of the task

The experiment was a self-paced information-passing task with nine blocks, conceptually similar to the internal validation task. Each block consisted of the same set of 20 trivia questions (e.g., What is the main component of the Martian atmosphere?) in a randomized order. We instructed the participants to pass an answer to another player considering the reward units and his or her past performance. In each trial, correct and incorrect answers were shown separately on the corner of the screen. The correct answer was marked by a black circle. Apart from the correct answer, the monetary reward of each choice and how many times participants had chosen this choice in the former blocks were also provided. To induce participants to make a trade-off between money and honesty, a higher reward was set for the incorrect answer in over 60% of trials. Participants had 4 s to make a response, feedback was shown after the choice and lasted for 1 s. At the end of each finished block, the cumulative monetary reward of the block would be displayed

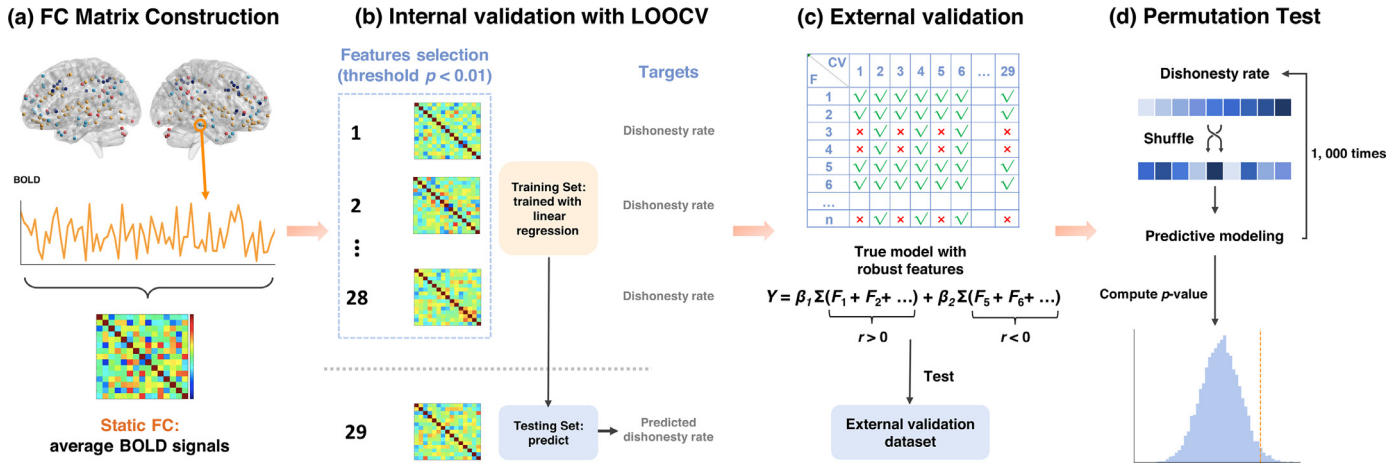

Fig. 2. Workflow for Connectome-based Predictive Modeling. (a) FC matrix construction. The time series of every brain region in the Power atlas was extracted and averaged (Power et al., 2011). Brain regions that overlap with one or more social brain networks were preserved to construct the FC matrix. FC between each pair of ROIs was obtained by Pearson correlation of the averaged time series. A 112-by-112 FC matrix was constructed for each participant in the internal and external validation dataset. (b) Internal validation with LOOCV. Specifically, feature selection was applied to filter out FCs that might contribute to the prediction. Note that the feature selection was only used to training sets of the internal validation dataset. Then, linear regression was used to train the summed strength of FC from $N - 1$ participants; the trained linear regression model was tested on the left-out one participant and output a predicted dishonesty rate. (c) External validation. Features that appeared every time of the internal cross-validation were treated as robust features to build a true model. This true model was trained on all samples of the internal validation dataset and tested on the external validation dataset. Abbrev.: CV, cross-validation; F, feature.(d) Permutation test for statistics. The significance of prediction was evaluated with 1000 permutations.

on the screen. Same as the internal validation task, trials with a higher reward for the wrong answer to motivate dishonesty were defined as the dishonest condition. The dishonesty rate was defined as the proportion of false answers delivered in all trials.

2.2.3. MRI acquisition

All MRI data were acquired using a 3.0 T Siemens MAGNETOM Prisma MRI scanner with a 64channel head coil at the Center for Cognitive and Brain Sciences at the University of Macau. Highresolution T1-weighted images were acquired for each participant at first (3D MPRAGE sequence; voxel size = 1 × 1 × 1 mm^3; FOV = 256 mm; 176 slices, slice thickness: 1 mm; TR = 2300 ms, TE = 2.26 ms, flip angle = 8°). Eight-minute rsfMRI data was collected by an echo-planar imaging (EPI) sequence before the task (voxel size = 2 × 2 × 2 mm^3; FOV = 256 mm; 63 slices, slice thickness: 2 mm; TR = 1000 ms, TE = 30 ms, flip angle = 90°).

2.3. fMRI preprocessing

The rsfMRI preprocessing was performed using the advanced DPARSF module V5.1 (Yan et al., 2016). The first ten volumes were discarded due to the instability of the MRI signal. Then, all volume slices were corrected for different signal acquisition times, following each participant's time series of images. Individual structural images (T1-weighted MPRAGE) were co-registered to the mean functional image after realignment. The transformed structural images were segmented into the gray matter (GM), the white matter (WM), and cerebrospinal fluid (CSF) (Ashburner and Friston, 2005). To remove the nuisance signals, the Friston 24-parameter model (Friston et al., 1996) was utilized to regress out head motion, as well as the mean WM and CSF signals. The functional data from individual native space was transformed to the standard Montreal Neurological Institute (MNI) space (http://www.bic.mni.mcgill.ca/ServicesAtlases/HomePage). Spatial smoothing (FWMH kernel: 6 mm) was applied to the functional images for the connectivity analysis. Further, temporal filtering (0.01–0.1 Hz) was performed on the time series. The preprocessing of the rsfMRI data remained the same for both the internal and external validation datasets. The only difference was that we skipped slice timing for the external validation dataset as the TR is less than 2000 ms.

2.4. CPM: support vector regression

The workflow of CPM analysis was presented in Fig. 2. The FC matrix construction was conducted in the DPARSF toolbox. First, we extracted the BOLD time series of 264 regions in the whole brain according to the Power's atlas (Power et al., 2011). The 264 brain regions in the Power's atlas were divided into 14 brain networks. Since some of the networks were assumed to be irrelevant with dishonesty, such as auditory, visual, and sensory-somatomotor networks, we limited the CPM analysis to regions that overlap with brain networks crucial to social cognition. Then, we obtained four association test masks from Neurosynth (https://neurosynth.org/) using the following keywords, respectively: reward, selfreferential, moral, and cognitive control. Due to the overlap between these networks, the same brain region in the atlas may belong to multiple brain networks. To solve this problem, we calculated the averaged Z-score (from a two-way ANOVA of Neurosynth) of each mask within one brain region as supplementary evidence for ROI classification. For example, if an ROI had a higher Z-score for the reward network than the self-referential network, we would attribute it to the reward network. After the reduction, 48 ROIs were preserved due to the overlap with the reward network, 29 ROIs were preserved due to the overlap with the self-referential network, 18 ROIs were preserved due to the overlap with the moral network, and 17 ROIs were preserved due to the overlap with the cognitive control network. Finally, 112 ROIs were used to construct the FC matrix. A 112-by-112 FC matrix was obtained by Pearson's correlation between the averaged BOLD time series of each pair of ROIs. Fisher's Z transform was performed on Pearson's correlation coefficient (r). The static FC matrix was calculated participant by participant, resulting in 29 FC matrices of the internal validation dataset and 25 FC matrices of the external validation dataset.

Then, we implemented a linear regression model to the internal validation dataset to predict individuals' dishonesty rate using leave-one-out cross-validation (LOOCV) (Beaty et al., 2018; Dosenbach et al., 2010; Finn et al., 2015; Marek et al., 2022; Tipping, 1999). For each iteration of LOOCV, participants were divided into training sets with 28 samples (N - 1) and test sets with the left one sample. Following previous studies (Beaty et al., 2018; Shen et al., 2017), only features that had a significant association with behavioral indicators would be preserved for the prediction. We conducted Pearson correlation between every FC in the 112-by-112 matrix and the dishonesty rate for each training set. The cri-

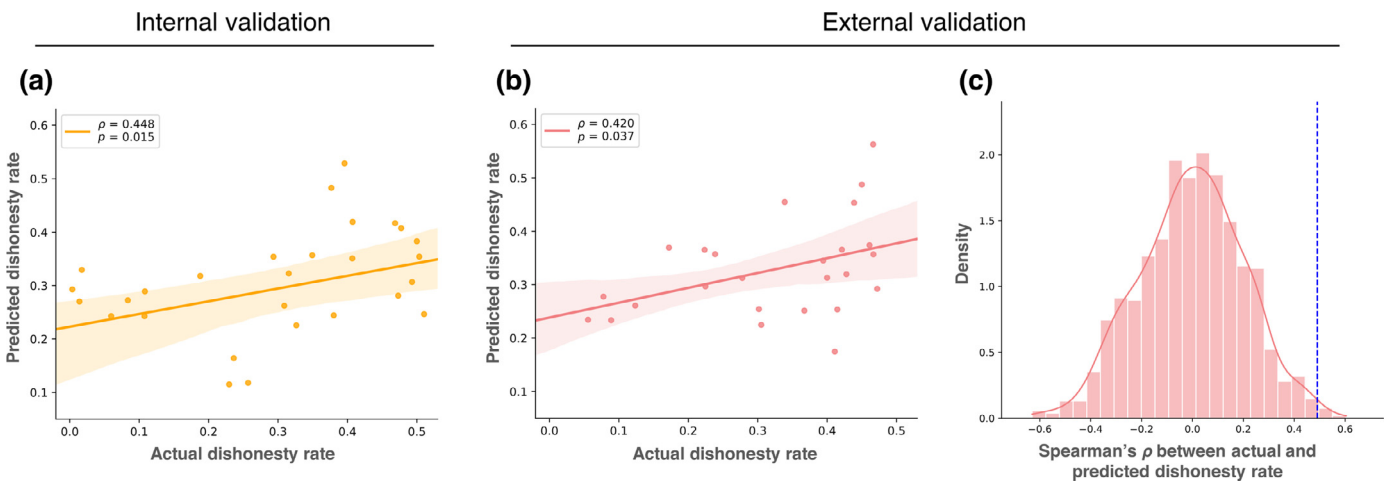

Fig. 3. Performance of CPM on dishonesty prediction. (a) The Spearman correlation between the observed dishonesty rates and the predicted dishonesty rates of the internal validation. (b) The Spearman correlation between the observed dishonesty rates and the predicted dishonesty rates of the external validation. (c) The null distribution of the external validation Spearman's ρ values after 1000 permutations of the internal validation dataset. The dashed blue line indicates Spearman's ρ of the true model. The permutation test resulting p value is 0.012.

terion for feature selection was that the FC should be significantly correlated to the dishonesty rate with a threshold $p < 0.01$ (Rosenberg et al., 2016; Takagi et al., 2018). Note that feature selection was applied to only the training sets to obtain relatively sparse features. Strengths of selected FCs were summed by significant positive or negative associations (i.e., Pearson correlation's $r > 0$ or $r < 0$) with the dishonesty rate into two variables, which were then used as predictors in the linear regression model. LOOCV was performed 29 times (N), with each participant being the test sample once and resulting in 29 predicted dishonesty rates. Finally, the Spearman correlation's ρ and p value between observed dishonesty rates and predicted dishonesty rates were used to evaluate model performance, along with the mean squared error (MSE).

To test if the model of the internal validation dataset could be generalized to new samples, we performed an external validation. Due to the LOOCV procedure described above, the selected features of each iteration were slightly different. Therefore, we kept features that appeared in all 29 times of cross-validation to build a robust true model (Bellucci et al., 2019; Shen et al., 2017). For example, as in Fig. 2c, we would exclude feature number 3 and number 4 for further analysis since they were not selected in cross validation number 1, 3, 5. We trained a model using these robust features on all samples of the internal validation dataset and obtained coefficients for the two predictors (summed positive FC strength and summed negative FC strength). The same model with fixed features and coefficients were applied to each participant of the external validation dataset. Similarly, the Spearman correlation and MSE were used to verify the true model (Fig. 2, Fong et al., 2019; Ngo et al., 2022; Rosenberg et al., 2016; Takagi et al., 2018).

Permutation tests were used to evaluate the statistical significance of the predictive model. Specifically, the observed dishonesty rates from all participants in the internal validation dataset were randomly shuffled 1000 times. For each time of permutation, the entire process of the internal validation was repeated with shuffled data. The predictive model derived from shuffled data would be tested on each participant of the external validation dataset and output a predicted dishonesty rate. Then we calculated the Spearman correlation coefficient (ρ) between the predicted and observed dishonesty rates. Finally, we counted the number of ρ values from the 1000 permutations greater than the real ones from the true model and divided it by the times of permutation (1000), obtaining the p value of the permutation test (Poldrack et al., 2020; Scheinost et al., 2019; Speer et al., 2022; Zuo et al., 2019).

To figure out which network or network pair contributes most to dishonesty, we counted the number of preserved edges in the predictive model for each network pair. Inspired by previous studies (Dosenbach et al., 2010; Speer et al., 2022), we also performed an iterative analysis to assess the importance of features. For each time of iteration, we excluded one column of FC from the feature space and retrained the model using the rest of FCs. Then we calculated the difference between the performance (correlation between predicted and observed values) of the true model and the incomplete model. Finally, differences with the same number of preserved FCs were ranked as feature importance. The original feature importance ranged from -0.04 to 0.07 (true model performance - incomplete model performance), the higher the more important. For the convenience of visualization, we enlarged the original feature importance by standardizing them. The results were visualized in a 4-by-4 matrix, with each entry denoting a network pair. Except for the concentrated four social brain networks, the 112 ROIs also belong to one of the 14 basic networks of the pre-defined Power's atlas. For the need of comparison, we also visualized the feature importance in a 11-by-11 matrix using Power's atlas. Note that three of the 14 brain networks were excluded as these networks did not overlap with the selected ROIs completely.

3. Results

3.1. Behavioral results

The motivated dishonesty rate of 29 participants in the internal validation dataset ranged from 0.004 to 0.51 (mean ± SD = 0.30 ± 0.16). The motivated dishonesty rate of 25 participants in the external validation dataset ranged from 0.056 to 0.47 (mean ± SD = 0.32 ± 0.14). The distributions of the dishonesty rate in each dataset were shown in Fig. 1c and d, and both samples manifested pronounced individual differences. For debrief questions in both datasets, all participants declared they did not doubt the cover story and did not know the true purpose of the experiment.

3.2. CPM results

We used CPM to examine the degree to which the rsFC of certain social cognitive brain regions could predict dishonesty. Correlation matrices for static FC were built, respectively, and a linear regression model was selected for training. For the internal validation, the model was trained on N - 1 participants and tested on the left-out participant of the internal validation dataset. For the external validation, the model was trained on all participants of the internal validation dataset and tested on samples of the external validation dataset. The internal validation demonstrated that summed strength of selected FCs can significantly predict the dishonesty rate of participants (Fig. 3a; $\rho = 0.448$, $p = 0.015$,

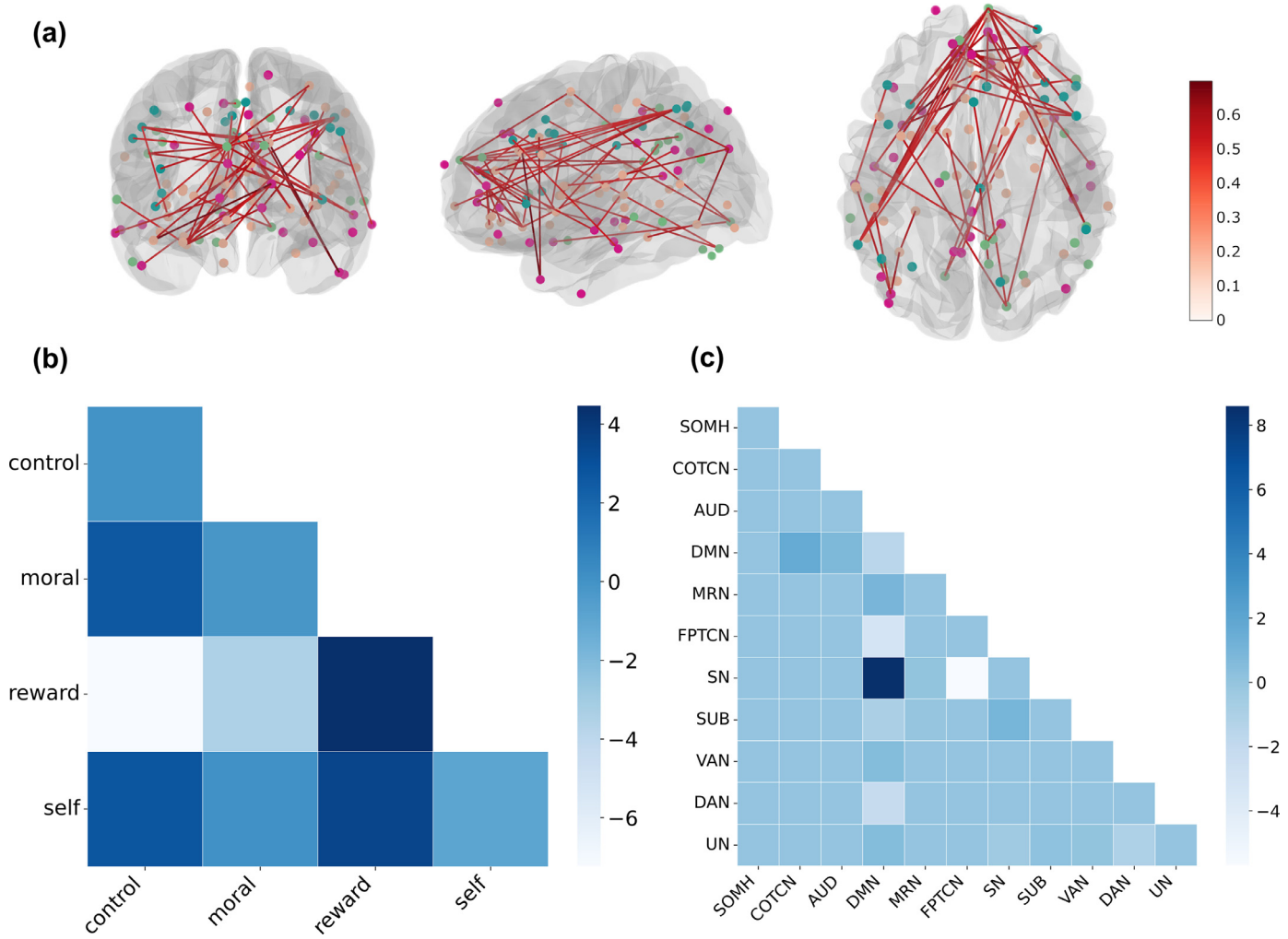

Fig. 4. Visualization of CPM results. (a) All selected features in the predictive model were presented from three views. Nodes from different social networks were marked with different colors: dark cyan, green, pink, and purple represent cognitive control network, moral network, reward network, and self-referential network, respectively. Color bar represents the strength of association between features and the dishonesty rate. (b) According to the four social brain networks, the standardized feature importance within and between the same pair of networks were summed and visualized in a 4-by-4 coefficient matrix. *Abbrev.*: control, cognitive control network; self, self-referential network. (c) According to the network partition of Power's atlas, the standardized feature importance within and between the same pair of networks were summed and visualized in a 11-by-11 coefficient matrix. *Abbrev.*: SOMH, somatomotor hand network; COTCN, cingulo-opercular task control network; AUD, auditory network; DMN, default mode network; MRN, memory retrieval network; FPTCN, fronto-parietal task control network; SN, salience network; SUB, subcortical network; VAN, ventral attention network; DAN, dorsal attention network; UN, uncertain.

$MSE = 0.028$). The fixed model from the internal validation dataset was then tested on the external validation dataset. Similarly, the Spearman correlation between observed and predicted dishonesty rate resulted in $\rho = 0.420$ with significant level $p = 0.037$, $MSE = 0.016$ (Fig. 3c). We noticed that all preserved features in the true model were positively correlated with the dishonesty rate, thus there was only one coefficient for the summed positive FC strength in the true model. To keep in line with previous research schema (Beaty et al., 2018; Shen et al., 2017), we retained the negative association part of the model in our CPM workflow (Fig. 2c). The permutation test was conducted to examine the significance of the true model. It demonstrated that the predictive power of the true model is significantly greater than the chance level ($p = 0.012$, Fig. 3b), which means in the 1000 times of permutation only 12 times the model worked out better on the shuffled data than the observed data. To summarize, the model built on the internal validation dataset could be generalized to the external validation dataset, indicating that the summed strength of preserved FCs in the true model is highly predictive of the dishonesty rate.

All selected FCs in the true model were presented in Fig. 4a through Nilearn (Abraham et al., 2014). To better understand the predictive model of the CPM analysis, we visualized the number of selected edges within and between networks according to the two attributions of each ROI (the four social networks and the Power's networks, see Fig. S3). The result demonstrated that all social brain networks contribute to the prediction of dishonesty rate, especially FCs between reward and self-referential networks (12 edges). Moreover, an iterative analysis was conducted to compare the importance of different features. Standardized feature importance for edges connecting the same pair of networks were summed. According to the four social networks, the summed importance was higher for edges within the reward network and edges connecting reward and self-referential networks (Fig. 4b). Similarly, the Power's matrix showed that FCs between DMN and salience network (SN) play an essential role in predicting dishonesty (Fig. 4c). Comparing the counting matrix with the feature importance matrix, we noticed that although more preserved features belong to connections between reward and self-referential networks, edges within re-

ward network showed higher feature importance. This result indicated that feature importance should be taken into account in addition to quantity.

To confirm our hypothesis that rsFC of social brain regions are predictive of dishonest behavior and complement the CPM results, we further performed the ROI-based analysis and provided the results in supplementary materials (Fig. S4 and Table S1).

4. Discussion

The present study investigated whether rsFC can predict individuals' motivated dishonesty, with two datasets. For both datasets, we designed the information passing task with monetary reward temptation, and collected rsfMRI data before the task. The correlation analyses between individuals' intrinsic FC and the spontaneous lying rate demonstrated that the rsFC of social networks can predict motivated dishonesty. Our work provides additional evidence linking individuals' dishonest behavior and rsFC in critical cognitive networks, in line with previous studies (Greene and Paxton, 2009; Speer et al., 2022; Yin et al., 2021; Yin and Weber, 2019).

The results of the CPM analysis suggest that the strength of FCs within and between the four social brain networks (i.e., reward, self-referential, moral, and cognitive control networks) can predict dishonesty. Among all selected features in the CPM, FCs within the reward network and FCs between reward and self-referential networks showed the most considerable contribution. These findings are consistent with previous studies (Sai et al., 2021; Speer et al., 2020; Yin et al., 2021). For example, a meta-analyses research summarized 58 neuroimaging studies and found that spontaneous dishonesty consistently activate pregenual ACC and VLPFC, which are closely associated to reward and social cognition. A cross-age research has proved that FC between caudate (regarded as reward-related brain region) and mPFC (regarded as self-related brain region) can predict variations of self-reported trait honesty (Yin et al., 2021). Another study using CPM revealed that individuals' dishonest decisions are associated with the strength of FCs between the self-referential and reward networks (Speer et al., 2020). Compared with above-mentioned studies, we used a different kind of paradigm to measure participants' motivated dishonest behavior, named sender-receiver paradigm. Our findings replicated main results of these studies that self-related and reward-related brain regions support dishonest behavior. Moreover, our findings highlighted the role of cognitive control network in predicting motivated dishonesty. In addition, the method we obtain FC among social brain regions enabled us to intuitively compare contributions from the perspective of large-scale brain networks.

4.1. Reward network in dishonesty prediction

As one drive to motivated unethical behaviors, monetary rewards is commonly used to induce selfinterest related moral decisions (FeldmanHall et al., 2012). In both tasks of the internal and external validation dataset, we used monetary rewards to induce spontaneous dishonesty. As a result, the functional coupling within the reward network maps out individuals' sensitivity to money, which profoundly influences dishonest behavior. These results echo previous work indicating that neural response to anticipated reward can predict dishonesty in another independent task (Abe and Greene, 2014). Our recent work addressed that honesty or dishonesty default depends on the self-interest (Wu et al., 2021), honest responses are slower for selfish people since it is harder for them to resist the monetary temptation. Combined with previous works showing value representation is foundation of dishonesty (Gross et al., 2014; Wang et al., 2014; Gazit et al., 2020), the increased FCs in the reward network may imply that the stronger encoding of the rewards, the more motivated dishonest behavior.

4.2. DMN in dishonesty prediction

FC related to self-referential network is highly predictive of dishonest decisions as well. Based on Power's atlas(Power et al., 2011), FCs within the DMN have a dominant effect in the prediction. Given the prominent role of the DMN in generating internally-direct thought and processing self-related information, it proves the importance of self-related neural activity in predicting dishonesty (Molnar-Szakacs and Uddin, 2013; Qin and Northoff, 2011). Furthermore, FC between reward and self-referential networks may reflect that the reward representation is modulated by self-awareness (Ross et al., 2011; Speer et al., 2020). Participants with solid self-awareness have stronger motivation to maintain self-image and resist temptation (Yin et al., 2021). In keeping with that, the increased FC between reward and self-referential networks indicates the process of balancing between reward and self-worth. Moreover, self-awareness forces individuals to behave under moral code and social norms, resulting in strengthened FC between self-referential and moral networks.

4.3. Cognitive control network in dishonesty prediction

Consistent with previous work, our findings showed that the neural activity of the cognitive control network affects the prediction by links with the other three social networks. Several lines of evidence support these links. Theoretically, lying requires the recruitment of cognitive resources to solve the conflicts between money temptation, self-image, and moral norm (Van't Veer et al., 2014). Since the cognitive control network is related to executive function, including conflict monitoring and resolution, frequent lying may result in a greater likelihood of exerting top-down control on other related cognitive networks (Brydges et al., 2020; Jiang et al., 2018; Marek and Dosenbach, 2018; Van't Veer et al., 2014; Wang et al., 2010). Also, it was found that the cognitive control network may play a role in rationalization to resolve cognitive dissonance (Jarcho et al., 2011). Therefore, the strengthened FCs between cognitive control and the other three networks may be associated with more dishonesty by resolving the moral conflict and rationalizing the dishonesty. These findings further accentuate the close association between the increased connectivity of the four social cognitive networks and human's adaptive dishonesty.

4.4. Replicable effect from rsFC to dishonesty prediction

To deal with the recent concern on the reproducibility and replicability of neuroimage studies, much efforts and attempts in developing workflows, tools, and guidelines that aim to increase them in research have been made (Dosenbach et al., 2017; Kundu et al., 2012; Marek et al., 2022). Since obtaining MRI data remains expensive and acquiring big sample size is difficult for rarer clinical conditions, small-sample neuroimaging will always be critical for studying the human brain (Marek et al., 2022). Our work, contributes to this field as one practices that can be implemented in other labs worldwide, which is to reproduce previous findings in different samples, different cultures, different tasks, though with small sample size. A critical consideration relating to small sample size is the statistical power, however, the replication study with prior hypothesis and cross validation can still contribute evidence and confirm existing findings (Scheinost et al., 2019). Although it is hard to define "successful" replication with small sample size, our results largely overlap with previous studies in predicting dishonesty (Speer et al., 2022; Yin et al., 2021).

4.5. Limitations of the current study

There are several limitations in the current study. First, the behavioral tasks in both the internal and external validation datasets (Fig. 1) are more complex than common paradigms. Participants cannot lie in private but have to deceive others for more rewards, which may lead

them to be distracted by self-evaluation (Cui et al., 2018). Without post-checking of the awareness of possible dishonesty after the task, it makes the interpretation or inference of the propensity of dishonesty harder in individuals with low lie rate or not lied at all. We have excluded three participants with zero dishonesty rate in the external validation dataset. After including these three participants, the generalizability of the model went worse ($\rho = 0.329$, $p = 0.088$). Second, FCs are measured by Pearson correlation which cannot reflect the directionality of the interactions between brain regions, thus our findings cannot reveal the causal effects of FCs on dishonesty either. Most importantly, although we did external validation using another independent dataset and the true model survived the permutation test, the relatively small sample size may bring bias and variance to the model (Scheinost et al., 2019). According to the recent paper, a sample size of about 2000 is required for the reproducibility of models between rsFC and cognitive ability (Marek et al., 2022). Furthermore, this study only focused on the cognitive system of dishonesty while ignoring the emotion system. According to previous studies, individuals cannot avoid emotion fluctuations in the process of lying, therefore emotion could be an important indicator of lie detection (Greene and Haidt, 2002; Moll et al., 2002). How the cognition and emotion systems interact in the process of lying and whether these interactions can be manifested at the neural level remains to be explored in the future.

5. Conclusion

In summary, the CPM analysis across two datasets demonstrated that FC during resting-state can predict dishonesty. Increased FCs within the reward network and between reward and self-referential networks can strongly predict dishonesty, indicating top-down control of self-related processing. The results reflect an essential role of social brain regions in promoting dishonest behavior and such effect is reproducible in several studies.

Data and code availability statement

The data used in this manuscript is not available due to privacy issues. The code used in this manuscript is available at https://github.com/andlab-um/restDishonesty.

Declaration of Competing Interest

All authors declare no competing interests.

Credit authorship contribution statement

Luoyao Pang: Methodology, Formal analysis, Writing – original draft, Writing – review & editing. **Huidi Li:** Methodology, Formal analysis, Writing – original draft, Writing – review & editing. **Quanying Liu:** Writing – original draft. **Yue-Jia Luo:** Supervision. **Dean Mobbs:** Project administration. **Haiyan Wu:** Investigation, Funding acquisition, Writing – original draft, Writing – review & editing, Supervision.

Acknowledgment

This work is funded by the National Natural Science Foundation of China (U1736125), University of Macau (CRG2020-00001-ICI, SRG202000027-ICI), Natural Science Foundation of Guangdong Province (2021A1515012509, 2019A1515111038), the Science and Technology Development Fund (FDCT) of Macau (0127/2020/A3), and Shenzhen-Hong Kong-Macao Science and Technology Innovation Project (Category C) (SGDX2020110309280100). The authors would like to thank Mr Hao Yu who provided general support in participant recruiting. We would also like to thank Ms Xinyi Xu for the external validation dataset.

Supplementary materials

Supplementary material associated with this article can be found, in the online version, at doi:10.1016/j.neuroimage.2022.119253.

References

Abe, N., 2011. How the brain shapes deception: an integrated review of the literature. Neuroscientist 17, 560–574.
Abe, N., Greene, J.D., 2014. Response to anticipated reward in the nucleus accumbens predicts behavior in an independent test of honesty. J. Neurosci. 34, 10564–10572.
Abraham, A., Pedregosa, F., Eickenberg, M., Gervais, P., Mueller, A., Kossaifi, J., Gramfort, A., Thirion, B., Varoquaux, G., 2014. Machine learning for neuroimaging with scikit-learn. Front. Neuroinform. 8, 14.
Ashburner, J., Friston, K.J., 2005. Unified segmentation. Neuroimage 26, 839–851.
Bargh, J.A., Chartrand, T.L., 1999. The unbearable automaticity of being. Am. Psychol. 54, 462.
Beaty, R.E., Kenett, Y.N., Christensen, A.P., Rosenberg, M.D., Benedek, M., Chen, Q., Fink, A., Qiu, J., Kwapil, T.R., Kane, M.J., et al., 2018. Robust prediction of individual creative ability from brain functional connectivity. Proc. Natl. Acad. Sci. 115, 1087–1092.
Bellucci, G., Hahn, T., Deshpande, G., Krueger, F., 2019. Functional connectivity of specific restingstate networks predicts trust and reciprocity in the trust game. Cogn. Affect. Behav. Neurosci. 19, 165–176.
Bettus, G., Bartolomei, F., Confort-Gouny, S., Guedj, E., Chauvel, P., Cozzone, P.J., Ranjeva, J.-.P., Guye, M., 2010. Role of resting state functional connectivity mri in presurgical investigation of mesial temporal lobe epilepsy. J. Neurol. Neurosurg. Psychiatry 81, 1147–1154.
Biswal, B., Zerrin Yetkin, F., Haughton, V.M., Hyde, J.S., 1995. Functional connectivity in the motor cortex of resting human brain using echo-planar mri. Magn. Reson. Med. 34, 537–541.
Brydges, C.R., Barcel´o, F., Nguyen, A.T., Fox, A.M., 2020. Fast fronto-parietal cortical dynamics of conflict detection and context updating in a flanker task. Cogn. Neurodyn. 14, 795–814.
Buss, D.M., 2019. Evolutionary Psychology: The New Science of the Mind. Routledge.
Christ, S.E., Van Essen, D.C., Watson, J.M., Brubaker, L.E., McDermott, K.B., 2009. The contributions of prefrontal cortex and executive control to deception: evidence from activation likelihood estimate meta-analyses. Cereb. Cortex 19, 1557–1566.
Christov-Moore, L., Reggente, N., Douglas, P.K., Feusner, J.D., Iacoboni, M., 2020. Predicting empathy from resting state brain connectivity: a multivariate approach. Front. Integr. Neurosci. 14, 3.
Crockett, M.J., Siegel, J.Z., Kurth-Nelson, Z., Dayan, P., Dolan, R.J., 2017. Moral transgressions corrupt neural representations of value. Nat. Neurosci. 20, 879–885.
Cui, F., Wu, S., Wu, H., Wang, C., Jiao, C., Luo, Y., 2018. Altruistic and self-serving goals modulate behavioral and neural responses in deception. Soc. Cogn. Affect. Neurosci. 13, 63–71.
DePaulo, B.M., Lindsay, J.J., Malone, B.E., Muhlenbruck, L., Charlton, K., Cooper, H., 2003. Cues to deception. Psychol. Bull. 129, 74.
Dosenbach, N.U., Koller, J.M., Earl, E.A., Miranda-Dominguez, O., Klein, R.L., Van, A.N., Snyder, A.Z., Nagel, B.J., Nigg, J.T., Nguyen, A.L., et al., 2017. Real-time motion analytics during brain MRI improve data quality and reduce costs. Neuroimage 161, 80–93.
Dosenbach, N.U., Nardos, B., Cohen, A.L., Fair, D.A., Power, J.D., Church, J.A., Nelson, S.M., Wig, G.S., Vogel, A.C., Lessov-Schlaggar, C.N., et al., 2010. Prediction of individual brain maturity using fMRI. Science 329, 1358–1361.
Farah, M.J., Hutchinson, J.B., Phelps, E.A., Wagner, A.D., 2014. Functional mri-based lie detection: scientific and societal challenges. Nat. Rev. Neurosci. 15, 123–131.
FeldmanHall, O., Dalgleish, T., Thompson, R., Evans, D., Schweizer, S., Mobbs, D., 2012. Differential neural circuitry and self-interest in real vs hypothetical moral decisions. Soc. Cogn. Affect. Neurosci. 7, 743–751.
Finn, E.S., Shen, X., Scheinost, D., Rosenberg, M.D., Huang, J., Chun, M.M., Papademetris, X., Constable, R.T., 2015. Functional connectome fingerprinting: identifying individuals using patterns of brain connectivity. Nat. Neurosci. 18, 1664–1671.
Fong, A.H.C., Yoo, K., Rosenberg, M.D., Zhang, S., Li, C.-S.R., Scheinost, D., Constable, R.T., Chun, M.M., 2019. Dynamic functional connectivity during task performance and rest predicts individual differences in attention across studies. Neuroimage 188, 14–25.
Friston, K.J., Williams, S., Howard, R., Frackowiak, R.S., Turner, R., 1996. Movement-related effects in fmri time-series. Magn. Reson. Med. 35, 346–355.
Fu, G., Lee, K., 2007. Social grooming in the kindergarten: the emergence of flattery behavior. Dev. Sci. 10, 255–265.
Gazit, T., Gonen, T., Gurevitch, G., Cohen, N., Strauss, I., Zeevi, Y., Yamin, H., Fahoum, F., Hendler, T., Fried, I., 2020. The role of mpfc and mtl neurons in human choice under goal-conflict. Nat. Commun. 11, 1–12.
Greene, J., Haidt, J., 2002. How (and where) does moral judgment work? Trends Cogn. Sci. 6, 517–523 (Regul. Ed.).
Greene, J.D., Paxton, J.M., 2009. Patterns of neural activity associated with honest and dishonest moral decisions. Proc. Natl. Acad. Sci. 106, 12506–12511.
Gross, J., Woelbert, E., Zimmermann, J., Okamoto-Barth, S., Riedl, A., Goebel, R., 2014. Value signals in the prefrontal cortex predict individual preferences across reward categories. J. Neurosci. 34, 7580–7586.
Haidt, J., 2001. The emotional dog and its rational tail: a social intuitionist approach to moral judgment. Psychol. Rev. 108, 814.
Hughes, B.L., Beer, J.S., 2013. Protecting the self: the effect of social-evaluative threat on neural representations of self. J. Cogn. Neurosci. 25, 613–622.

Jarcho, J.M., Berkman, E.T., Lieberman, M.D., 2011. The neural basis of rationalization: cognitive dissonance reduction during decision-making. Soc. Cogn. Affect. Neurosci. 6, 460–467.
Jiang, J., Bailey, K., Xiao, X., 2018. Midfrontal theta and posterior parietal alpha band oscillations support conflict resolution in a masked affective priming task. Front. Hum. Neurosci. 12, 175.
Klapwijk, E.T., van den Bos, W., Tamnes, C.K., Raschle, N.M., Mills, K.L., 2021. Opportunities for increased reproducibility and replicability of developmental neuroimaging. Dev. Cogn. Neurosci. 47, 100902.
Kundu, P., Inati, S.J., Evans, J.W., Luh, W.-.M., Bandettini, P.A., 2012. Differentiating bold and non-bold signals in fmri time series using multi-echo epi. Neuroimage 60, 1759–1770.
Lewis, A., Bardis, A., Flint, C., Mason, C., Smith, N., Tickle, C., Zinser, J., 2012. Drawing the line somewhere: an experimental study of moral compromise. J. Econ. Psychol. 33, 718–725.
Li, N., Ma, N., Liu, Y., He, X.-.S., Sun, D.-.L., Fu, X.-.M., Zhang, X., Han, S., Zhang, D.-.R., 2013. Resting-state functional connectivity predicts impulsivity in economic decision–making. J. Neurosci. 33, 4886–4895.
Lin, Q., Rosenberg, M.D., Yoo, K., Hsu, T.W., O'Connell, T.P., Chun, M.M, 2018. Resting-state functional connectivity predicts cognitive impairment related to alzheimer's disease. Front. Aging Neurosci. 10, 94.
Marek, S., Dosenbach, N.U., 2018. The frontoparietal network: function, electrophysiology, and importance of individual precision mapping. Dialogues Clin Neurosci 20, 133.
Marek, S., Tervo-Clemmens, B., Calabro, F.J., Montez, D.F., Kay, B.P., Hatoum, A.S., Donohue, M.R., Foran, W., Miller, R.L., Hendrickson, T.J., et al., 2022. Reproducible brain-wide association studies require thousands of individuals. Nature 603, 654–660.
Moll, J., de Oliveira-Souza, R., Eslinger, P.J., Bramati, I.E., Mour˜ao-Miranda, J., Andreiuolo, P.A., Pessoa, L., 2002. The neural correlates of moral sensitivity: a functional magnetic resonance imaging investigation of basic and moral emotions. J. Neurosci. 22, 2730–2736.
Molnar-Szakacs, I., Uddin, L.Q., 2013. Self-processing and the default mode network: interactions with the mirror neuron system. Front. Hum. Neurosci. 7, 571.
Ngo, G.H., Khosla, M., Jamison, K., Kuceyeski, A., Sabuncu, M.R., 2022. Predicting individual task contrasts from resting-state functional connectivity using a surface-based convolutional network. NeuroImage 248, 118849.
Pezzulo, G., Zorzi, M., Corbetta, M., 2021. The secret life of predictive brains: what's spontaneous activity for? Trends Cogn. Sci. 25, 730–743.
Poldrack, R.A., Huckins, G., Varoquaux, G., 2020. Establishment of best practices for evidence for prediction: a review. JAMA Psychiatry 77, 534–540.
Pornpattananangkul, N., Zhen, S., Yu, R., 2018. Common and distinct neural correlates of self-serving and prosocial dishonesty. Hum. Brain Mapp. 39, 3086–3103.
Power, J.D., Cohen, A.L., Nelson, S.M., Wig, G.S., Barnes, K.A., Church, J.A., Vogel, A.C., Laumann, T.O., Miezin, F.M., Schlaggar, B.L., et al., 2011. Functional network organization of the human brain. Neuron 72, 665–678.
Qin, P., Northoff, G., 2011. How is our self related to midline regions and the default-mode network? Neuroimage 57, 1221–1233.
Raichle, M.E., 2011. The restless brain. Brain Connect 1, 3–12.
Ren, Z., Daker, R.J., Shi, L., Sun, J., Beaty, R.E., Wu, X., Chen, Q., Yang, W., Lyons, I.M., Green, A.E., et al., 2021. Connectome-based predictive modeling of creativity anxiety. Neuroimage 225, 117469.
Rosenberg, M.D., Finn, E.S., Scheinost, D., Papademetris, X., Shen, X., Constable, R.T., Chun, M.M., 2016. A neuromarker of sustained attention from whole-brain functional connectivity. Nat. Neurosci. 19, 165–171.
Ross, J., Anderson, J., Campbell, R., 2011. Situational changes in self-awareness influence 3-and 4-year-olds' self-regulation. J. Exp. Child. Psychol. 108, 126–138.
Sai, L., Bellucci, G., Wang, C., Fu, G., Camilleri, J.A., Eickhoff, S.B., Krueger, F., 2021. Neural mechanisms of deliberate dishonesty: Dissociating deliberation from other control processes during dishonest behaviors. Proceedings of the National Academy of Sciences 118.
Sai, L., Wu, H., Hu, X., Fu, G., 2018. Telling a truth to deceive: examining executive control and reward-related processes underlying interpersonal deception. Brain Cogn. 125, 149–156.
Scheinost, D., Noble, S., Horien, C., Greene, A.S., Lake, E.M., Salehi, M., Gao, S., Shen, X., O'Connor, D., Barron, D.S., et al., 2019. Ten simple rules for predictive modeling of individual differences in neuroimaging. Neuroimage 193, 35–45.
Shen, X., Finn, E.S., Scheinost, D., Rosenberg, M.D., Chun, M.M., Papademetris, X., Constable, R.T., 2017. Using connectome-based predictive modeling to predict individual behavior from brain connectivity. Nat. Protoc. 12, 506–518.
Shi, L., Sun, J., Xia, Y., Ren, Z., Chen, Q., Wei, D., Yang, W., Qiu, J., 2018. Large-scale brain network connectivity underlying creativity in resting-state and task fMRI: cooperation between default network and frontal-parietal network. Biol. Psychol. 135, 102–111.
Speer, S.P., Smidts, A., Boksem, M.A., 2020. Cognitive control increases honesty in cheaters but cheating in those who are honest. Proc. Natl. Acad. Sci. 117, 19080–19091.
Speer, S.P., Smidts, A., Boksem, M.A., 2022. Individual differences in (dis) honesty are represented in the brain's functional connectivity at rest. Neuroimage 246, 118761.
Sun, D., Chan, C.C., Hu, Y., Wang, Z., Lee, T.M., 2015. Neural correlates of outcome processing post dishonest choice: an fMRI and ERP study. Neuropsychologia 68, 148–157.
Takagi, Y., Sakai, Y., Abe, Y., Nishida, S., Harrison, B.J., Mart´ınez-Zalaca´ın, I., Soriano–Mas, C., Narumoto, J., Tanaka, S.C., 2018. A common brain network among state, trait, and pathological anxiety from whole-brain functional connectivity. Neuroimage 172, 506–516.
Tian, Y., Yang, L., Chen, S., Guo, D., Ding, Z., Tam, K.Y., Yao, D., 2017. Causal interactions in resting-state networks predict perceived loneliness. PLoS One 12, e0177443.
Tipping, M., 1999. The relevance vector machine. Advances in neural information processing systems 12.
Valk, S.L., Hoffstaedter, F., Camilleri, J.A., Kochunov, P., Yeo, B.T., Eickhoff, S.B., 2020. Personality and local brain structure: their shared genetic basis and reproducibility. Neuroimage 220, 117067.
Van't Veer, A., Stel, M., van Beest, I., 2014. Limited capacity to lie: cognitive load interferes with being dishonest. Judgm. Decis. Mak. 9, 199–206.
Wang, L., Liu, X., Guise, K.G., Knight, R.T., Ghajar, J., Fan, J., 2010. Effective connectivity of the fronto-parietal network during attentional control. J. Cogn. Neurosci. 22, 543–553.
Wang, Q., Luo, S., Monterosso, J., Zhang, J., Fang, X., Dong, Q., Xue, G., 2014. Distributed value representation in the medial prefrontal cortex during intertemporal choices. J. Neurosci. 34, 7522–7530.
Wu, H., Cao, S., Bai, C., Chen, K., et al., 2021. Moral by default? the dynamic tradeoffs between honesty and self-interest. PsyArXiv.
Wu, H., Hu, X., Fu, G., 2009. Does willingness affect the n2-p3 effect of deceptive and honest responses? Neurosci. Lett. 467, 63–66.
Yan, C.G., Wang, X.D., Zuo, X.N., Zang, Y.F., 2016. Dpabi: data processing & analysis for (resting-state) brain imaging. Neuroinformatics 14, 339–351.
Yin, L., Hu, Y., Dynowski, D., Li, J., Weber, B., 2017. The good lies: altruistic goals modulate processing of deception in the anterior insula. Hum. Brain Mapp. 38, 3675–3690.
Yin, L., Weber, B., 2019. I lie, why don't you: neural mechanisms of individual differences in self-serving lying. Hum. Brain Mapp. 40, 1101–1113.
Yin, L., Zhong, S., Guo, X., Li, Z., 2021. Functional connectivity between the caudate and medial prefrontal cortex reflects individual honesty variations in adults and children. Neuroimage 238, 118268.
Zuo, X.N., Biswal, B.B., Poldrack, R.A., 2019. Reliability and reproducibility in functional connectomics. Front. Neurosci. 13, 117.